

Contents lists available at ScienceDirect

### Computational Materials Science

journal homepage: www.elsevier.com/locate/commatsci



# MoS<sub>2</sub>-MX<sub>2</sub> *in*-plane superlattices: Electronic properties and bandgap engineering *via* strain



Xiangying Su\*, Hongling Cui, Weiwei Ju, Yongliang Yong, Qingxiao Zhou, Xiaohong Li, Fengzhang Ren

School of Physics & Engineering, Henan University of Science & Technology, 263, Kaiyuan Road, Luoyang 471023, China

#### ARTICLE INFO

Article history: Received 21 October 2016 Received in revised form 13 February 2017 Accepted 15 February 2017

Keywords:
Transition metal dichalcogenides in-plane superlattices
Electronic properties
Bandgap engineering
Biaxial strain
First principles calculation

#### ABSTRACT

Using density functional theory calculations, we performed a study of the electronic properties of transition metal dichalcogenides (TMDCs) *in*-plane superlattices MoS<sub>2</sub>-MX<sub>2</sub> (MX<sub>2</sub> = WS<sub>2</sub>, MoSe<sub>2</sub>). Particular attention has been focused on the bandgap engineering by applying biaxial strain. All the three superlattices show semiconducting characteristics retaining the direct bandgap character of TMDCs monolayer. Moreover, the bandgap can be widely tuned by applying biaxial strain and a universal semiconductor-metal (S-M) transition occur at a critical strain. Especially, the direct bandgap can also be modulated in a range by moderate strain. The shift of metal atoms *d* orbitals toward the Fermi level is mainly responsible for the bandgap variation although a different physical mechanism was induced by tensile and compressive strain. As a result MoS<sub>2</sub>-WS<sub>2</sub> heterostructure needs a bigger critical strain for S-M transition due to the bigger bandgap.

© 2017 Elsevier B.V. All rights reserved.

#### 1. Introduction

Layered transition metal dichalcogenides (TMDCs) materials have emerged as promising materials to complement graphene, not only because they possess similar layered structural characteristics but also monolayer TMDCs show a lot of mechanical, optical, chemical, thermal and electronic properties that are comparable to or better than those of graphene [1,2], for example, the monolayer MoS<sub>2</sub> based transistor exhibits a high room-temperature current on/off ratios of  $1 \times 10^8$  and mobility of  $200 \text{ cm}^2 \text{ v}^{-1} \text{ s}^{-1}$ , similar to the mobility of graphene nanoribbons [1]. Due to their distinct properties, TMDCs materials have potential applications in a wide range, such as in gas sensors [3], energy storage [4], optoelectronic devices [5] and field-effect transistors [6]. Furthermore, the properties of TMDCs materials can be modulated by many ways, e.g., strain engineering [7,8], external electrical field [9], alloying [10] or doping [11]. More recently, fabricating the van der Waals (vdW) heterostructures opens up a new avenue to tune the electronic properties [12-14]. The diverse characters of individual TMDCs monolayer offer promising candidates to further formation of various heterostructures for nanoscience and next generation nanophotonic and nanoelectronic devices [15,16]. Heterostructures assembled by vertical stacking of different TMDCs materials have been realized by the transfer of their as-grown or exfoliated

flakes [17,18]. At the same time, many theoretical calculations have been performed and tunable electronic properties have been obtained [19–21]. In addition, superlattices builded by interfacing alternating monolayer MoS<sub>2</sub> and other TMDCs monolayers have been studied and multiple quantum wells have been formed [22].

Though the electronic properties can be effectively tuned by stacking, there exists a defect, which is the direct bandgap characteristics lost. Among those vertical heterostructures reported only MoS<sub>2</sub>/WSe<sub>2</sub> heterobilayers maintains the direct bandgap character and a very small biaxial strain (1%) can turn it into an indirect semiconductor [23]. MoS<sub>2</sub>/MX<sub>2</sub> superlattices all show indirect bandgaps [22]. In the effort to retain the direct bandgap character of semi-conductive TMDCs monolayer, maybe the in-plane heterostructures could be constructed. Moreover, the in-plane heterostructures could also lead to interesting new properties and applications. Furthermore, some transition metal dichalcogenide monolayer alloys such as Mo<sub>1-x</sub>W<sub>x</sub>S<sub>2</sub> and Mo<sub>1-x</sub>W<sub>x</sub>Se<sub>2</sub> with different x values have been synthesized in experiment [24,25]. Based on these preparation technologies and the similarity of the structures, we think that the in-plane superlattice MoS<sub>2</sub>/MX<sub>2</sub> should be experimentally realized, too.

In the present work, we therefore provide a detailed description of the electronic properties of TMDCs *in*-plane superlattices by using first-principles calculations in the framework of density functional theory (DFT). Monolayer WS<sub>2</sub>, MoSe<sub>2</sub> and WSe<sub>2</sub> were chosen to form *in*-plane superlattices with the most studied MoS<sub>2</sub> described as MoS<sub>2</sub>-MX<sub>2</sub> (MX<sub>2</sub> = WS<sub>2</sub>, MoSe<sub>2</sub>, WSe<sub>2</sub>).

<sup>\*</sup> Corresponding author.

E-mail address: xiangyingsu@126.com (X. Su).

In addition, due to strain has been regarded as one of the best strategies to modulate the bandgap of monolayer TMDCs. We think that the effect of strain on the electronic properties of *in*-plane superlattices will also be interesting. Here, the influence of biaxial strain including tensile and compressive strain on the bandgaps of MoS<sub>2</sub>-MX<sub>2</sub> *in*-plane superlattices will be studied, too.

#### 2. Model and calculation methods

MoS<sub>2</sub>-MX<sub>2</sub> *in*-plane superlattice supercell was composed of 2 MoS<sub>2</sub> units and 2 MX<sub>2</sub> units as shown in Fig. 1. In order to obtain the optimum values of the lattice constant, the total energy of heterostructures as functions of the lattice constant a is shown in Fig. 1(b). The optimum values of the lattice constants of the three systems are 6.37 Å, 6.50 Å and 6.50 Å, respectively, just the average of the optimized lattice constants of  $2 \times 2$  supercells of the two components (6.36 Å, 6.38 Å, 6.64 Å, and 6.64 Å for MoS<sub>2</sub>, WS<sub>2</sub>, MoSe<sub>2</sub>, and WSe<sub>2</sub>, respectively).

All of the calculations, including the geometry optimization and electronic properties calculations were performed with the Vienna ab initio simulation package (VASP) [26-27], based on density functional theory (DFT) and projector-augmented-wave (PAW) potentials [28]. The Perdew-Burke-Ernzerhof (PBE) [29] version of generalized gradient approximation (GGA) was used to describe the electron exchange-correlation interactions. The geometric structures are relaxed until the forces have converged to 0.01 eV/Å and the convergence criteria for energy is  $10^{-6} \text{ eV}$ . The plane wave cutoff was set at 400 eV. A k-point sampling of  $7 \times 7 \times 1$  was used for the geometry optimization and a  $15 \times 15 \times 1$  Monkhorst-Pack mesh was set for static electronic structure calculations. A sufficient vacuum of 20 Å was employed to avoid interaction between periodic images of slabs in the zdirection. On the base of the optimized structures, a hybrid functional in the Heyd-Scuseria-Ernaerhof (HSE06) method was adopted to give more accurate bandgaps [30]. In order to assess the spin-orbital coupling (SOC) effects on electronic structures, PBE + SOC was also performed

#### 3. Results and discussion

#### 3.1. Stability of the supperlattices

The stability of the supperlattices can be judged by the formation energy that can be calculated by:

$$E_f = E_{SL} - 2E_{MoS_2} - 2E_{MX_2}$$

where  $E_{SL}$ ,  $E_{MoS_2}$  and  $E_{MX_2}$  are energies of the supperlattices, free-standing MoS<sub>2</sub> and MX<sub>2</sub> per formula unit, respectively. The calculated results are listed in Table 1 and the negative values indicate that the three systems are all stable.

Also, in order to further verify the structural stability, molecular dynamics (MD) simulations were performed at room temperature. The changes of bond lengths with the MD steps are shown in Fig. 2. Considering the symmetry structure, only the results of half bonds in the supperlattice are shown. During the entire MD simulation process of 2 ps with the time step of 1 fs, no bond breaking is observed for all the supperlattices, suggesting high stability of these supperlattices.

#### 3.2. Electronic structures of MoS<sub>2</sub>-MX<sub>2</sub> in-plane superlattices

The PBE band structures in Fig. 3 (left) revealed that all MoS<sub>2</sub>-MX<sub>2</sub> in-plane superlattices show semiconducting characteristics with a direct bandgaps and the conduction band minimum (CBM) and the valence band maximum (VBM) are both located at K point, similar to the semi-conductive TMDCs monolayer. No significant differences among the band structures of the three systems were observed but different bandgaps (see Table 1). The bandgap value is different from the constituent monolayer (1.67 eV, 1.80 eV, 1.45 eV and 1.52 eV for monolayer MoS<sub>2</sub>, WS<sub>2</sub>, MoSe<sub>2</sub> and WSe<sub>2</sub>, respectively), indicating significant potential for bandgap engineering by seamlessly stitching TMDCs monolayers. Previous works proved that SOC has important influences on electronic properties of TMDCs [31-33]. Here the band structures obtained by PBE + SOC are also shown in Fig. 3 (middle). We see that the bandgaps become smaller and SOC results in significant valence band splitting: 272 meV, 164 meV and 311 meV for MoS<sub>2</sub>-WS<sub>2</sub>, MoS<sub>2</sub>-MoSe<sub>2</sub> and MoS<sub>2</sub>-WSe<sub>2</sub> systems, respectively. However, compared to SOC unconsidered, the trend of the bandgap under strain is almost the same (see Fig. S1 (Supporting Information)). So, when study the effect of strain on the bandgap, SOC is insignificant. In addition, as we all know, the PBE functional generally underestimates the bandgap value. In order to improve the accuracy, the HSE06 functional was used and the relevant results are also expressed in Fig. 3 (right). It can be seen that all systems have the expected bigger bandgap. However, except for the bigger bandgap the band structures with the CBM and VBM are similar to those based on PBE computation. So, considering the high computational cost associated with HSE06 computation and in order to compare with previous results based on PBE calculation, the following calculations including the charge density and the band structure tuned by strain engineering were all based on PBE func-

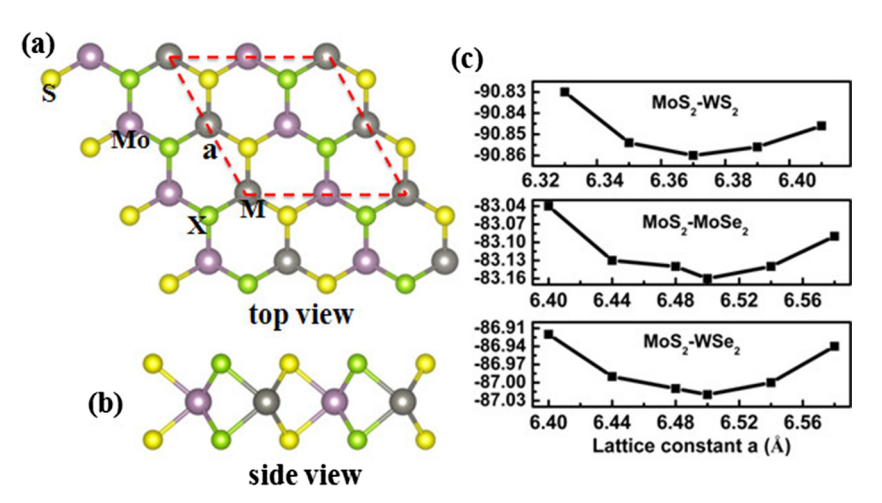


Fig. 1. (a) Top and (b) side views of TMDCs in-plane superlattices. (c) The total energy as a function of a lattice constant.

#### Download English Version:

## https://daneshyari.com/en/article/5453632

Download Persian Version:

https://daneshyari.com/article/5453632

Daneshyari.com